

Carrier cooling and exciton formation in GaSe

S. Nüsse, P. Haring Bolivar, and H. Kurz

*Institut für Halbleitertechnik II, Rheinisch-Westfälische Technische Hochschule Aachen, Sommerfeldstrasse 24,
D-52056 Aachen, Germany*

V. Klimov

Chemical Sciences and Technology Division, CST-6, MS J585, Los Alamos National Laboratory, Los Alamos, New Mexico 87545

F. Levy

Institut de Physique Appliquée, EPF Lausanne, CH-1015 Lausanne, Switzerland

(Received 27 February 1997)

The initial cooling of hot carriers and the subsequent exciton formation in GaSe are studied by time-resolved photoluminescence (PL) using femtosecond up-conversion techniques. From the time-resolved PL spectra of this layered III-VI semiconductor two different energy relaxation channels are derived. After an initial subpicosecond cooling due to Fröhlich-type interaction of carriers with longitudinal optical $E'(2^2)$ phonons a slower regime follows, which is dominated by deformation potential interaction with the nonpolar optical $A_1'(1^2)$ phonons. The coupling constant for nonpolar optical phonon scattering is derived. The subsequent formation of excitons is studied at different carrier densities and detection energies. A cross section for the free-exciton formation is determined based on a rate equation model. [S0163-1829(97)01132-6]

I. INTRODUCTION

Energy relaxation dynamics of hot carriers in semiconductors give important information on carrier-phonon interactions. These interactions affect critically such properties of the electronic system as carrier cooling and carrier mobilities, which directly determine the upper limits of operation frequencies of high speed switching devices. Therefore, time-resolved studies of dynamics of the coupled electron phonon system are of significant interest.

In polar semiconductors of high structural symmetry (III-V and II-VI compounds), the carrier phonon coupling is dominated by the long-range Fröhlich-interaction involving longitudinal optical phonons.¹⁻³ The situation is completely different in semiconductors with low site symmetry. In these compounds the short-range deformation potential coupling has a major influence on the carrier-phonon interaction, because of the large gradients of the atomic potentials.⁴ This is the case for the uniaxial layered semiconductor GaSe (Ref. 5) studied in the present paper. This material is much less investigated than tetrahedrally bound semiconductors. It is known from theoretical studies,⁶ Hall mobility,^{7,8} and absorption measurements,⁸⁻¹⁰ that the carrier-phonon interaction in GaSe is dominated by the deformation potential coupling to the nonpolar optical $A_1'(1^2)$ phonon mode (16.7 meV). From these type of studies values of the deformation potential constant D_{NPO} of 5.5–6.6 eV/Å were derived.^{6,8,10} However, so far only a few studies have been reported on the role of carrier-phonon interaction in the cooling of hot carriers photoexcited above the band gap of GaSe.¹¹⁻¹³ Most of the previous measurements were performed at room temperatures with a time resolution not better than 20 ps and at excitation densities clearly above the Mott-transition density in GaSe ($n_{\text{Mott}} \sim 5 \times 10^{17} \text{ cm}^{-3} - 10^{18} \text{ cm}^{-3}$).^{14,15} As a consequence, screened values of the deformation potential con-

stant were determined, which were several times smaller than the value reported in Refs. 6,8,10.

As the carrier energy during the cooling process reduces to values which are smaller than the exciton binding energy, the attractive Coulomb force between electrons and holes can bind them into excitons. As a result, the excitonic state gets incoherently occupied by thermalized electron hole pairs. Recently, exciton formation dynamics have been actively investigated in bulk GaAs and GaAs/Al_xGa_{1-x}As heterostructures.¹⁶⁻²¹ However, only little work has been done on III-VI materials such as GaSe. Most of the time-resolved measurements of exciton dynamics in GaSe show the formation of bound excitons due to localization of free excitons at layer stacking faults.²²⁻²⁵

In the present paper we study the carrier cooling dynamics at the band edge of GaSe with femtosecond time resolution in the regime of low excitation densities. These studies help to clarify ultrafast carrier cooling mechanisms in GaSe, which have not been yet investigated because of the limited time resolution in previous studies. Special attention is paid to the role of the $A_1'(1^2)$ phonon mode (16.7 meV) in the carrier cooling in case of negligible screening by the photoexcited carriers.

We study the dynamics of photoexcited carriers all the way through carrier cooling to the formation of free excitons and their final localization. The cross section for free exciton formation is derived by modeling PL time transients²⁶ recorded at different pump fluences. Additionally, we study exciton relaxation dynamics due to trapping at structural defects.

The paper is organized in the following way. In Sec. II the material system of GaSe and the experimental setup are described. In Sec. III the experimental results for the carrier cooling (Sec. III A) and the exciton formation (Sec. III B) are presented. Finally the conclusions are given in Sec. IV.

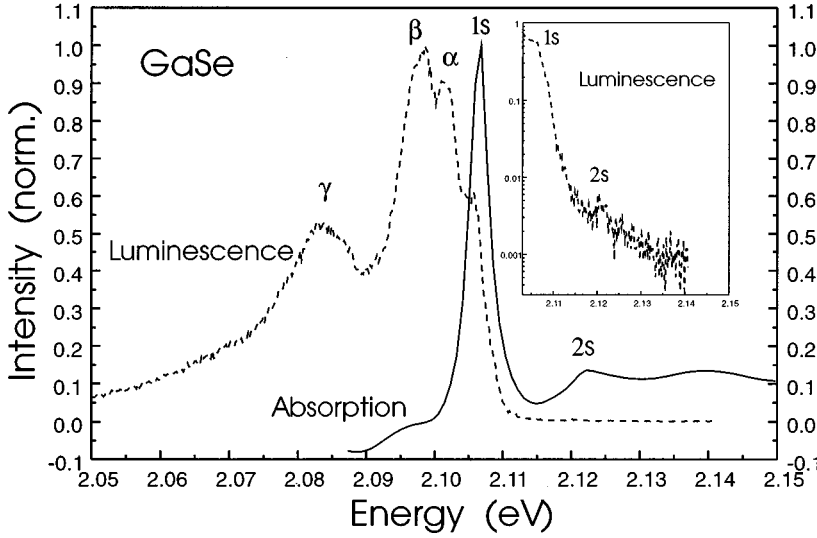


FIG. 1. Band-edge cw luminescence of GaSe (dashed line; inset: logarithmic plot; the cryostat temperature T is 10 K) in comparison to the linear absorption spectrum (solid line; $T=40$ K). The free-exciton resonances are marked as $1s$ and $2s$, and $\alpha-\gamma$ mark the spectral positions of bound excitons localized at stacking faults.

II. MATERIAL SYSTEM AND EXPERIMENTAL SETUP

GaSe is a III-VI semiconductor with layered crystal structure.²⁷ The samples under investigation are thin slabs cleaved from a Bridgman grown ingot.²⁸ They are attached strainfree to a sapphire substrate and mounted in a closed-cycle cryostat.

The samples are excited at 3.1 eV by frequency-doubled 100 fs pulses derived from a Kerr-lens mode-locked Ti:sapphire laser. The density of photoexcited carriers is on the order of $5 \times 10^{16} \text{ cm}^{-3}$. This is at least an order of magnitude lower than in previously reported studies of carrier cooling in GaSe.¹¹⁻¹³

The luminescence from the sample is collected in a backward geometry and is up-converted in a nonlinear β -barium borate crystal using a delayed laser pulse at the lasers fundamental frequency. The sum-frequency signal is dispersed in a double monochromator, and detected with a cooled photomultiplier coupled to a single photon counting system. The photoluminescence (PL) up-conversion technique has a time resolution of 150 fs. To improve the spectral resolution, some of the measurements were performed with picosecond laser pulses having narrower spectral bandwidth. These experiments nevertheless confirm only the analysis presented below and are not shown here.

The linear absorption spectrum (sample temperature T is 40 K) and the spectrum of time-integrated luminescence under pulsed excitation (cw luminescence) of GaSe are shown in Fig. 1. The $1s$ - and $2s$ -exciton direct gap resonances in GaSe are observed in linear absorption as pronounced peaks at 2.106 and 2.121 eV, respectively. The free-exciton lines are also well resolved in the cw luminescence. This indicates that the carrier density is below the Mott-transition density.^{15,29} The relatively large spacing between the direct $1s$ -exciton resonance and the direct band gap ($E_B^X = 19$ meV) in GaSe allows the clear separation of the exciton and free carrier dynamics in the femtosecond time-resolved PL measurements.

The luminescence experiments are performed at a sample temperature of 10 K. However, the exciton peaks in the linear absorption recorded at 40 and 50 K (the latter absorption spectrum is not shown here) have nearly the same spectral

positions as the corresponding peaks in the cw luminescence. These findings indicate that the sample temperature within the excited spot in the PL measurements is raised to approximately 45 K due to laser-induced heating.

Because of the layered structure of GaSe, stacking faults and dislocations can occur in the samples. Therefore, the cw luminescence from GaSe has several sample-dependent peaks below the free-exciton resonance (see Fig. 1). At low excitation densities (which is the case in the present studies) these peaks are mainly due to bound excitons localized at stacking faults in the sample.^{14,30}

GaSe is known as an indirect semiconductor with the lowest conduction-band minimum at the M point of the Brillouin zone. However, the energy separation of Γ and M conduction-band minima is not well known. The values reported in the literature deviate from 25 to 130 meV.^{14,31} No luminescence from the indirect gap is observed in the present studies in agreement with previous reported measurements.¹⁴

III. RESULTS AND DISCUSSION

A. Carrier cooling dynamics

Figure 2 shows time-resolved luminescence spectra of GaSe. For early times after optical excitation of the carriers the spectral maximum of the luminescence is located above the $1s$ -exciton resonance moving towards lower energies with longer time. The high-energy slope of the spectra becomes steeper with increasing time delay. At negative delay times the long-lived luminescence due to accumulated localized excitons is observed as a broadband at low energy (~ 2.08 eV). Essentially the same dynamics are obtained in measurements with improved spectral resolution using picosecond laser pulses. The recorded PL dynamics are related to the cooling of electrons and holes, the formation of excitons from the carriers as they lose energy to the phonon system and exciton trapping. In what follows, we use the time-resolved PL spectra to derive the relaxation rate related to the carrier cooling.

The PL above the band gap of GaSe ($E > E_{\text{gap}} = 2.125$ eV) results from the recombination of unbound electron hole

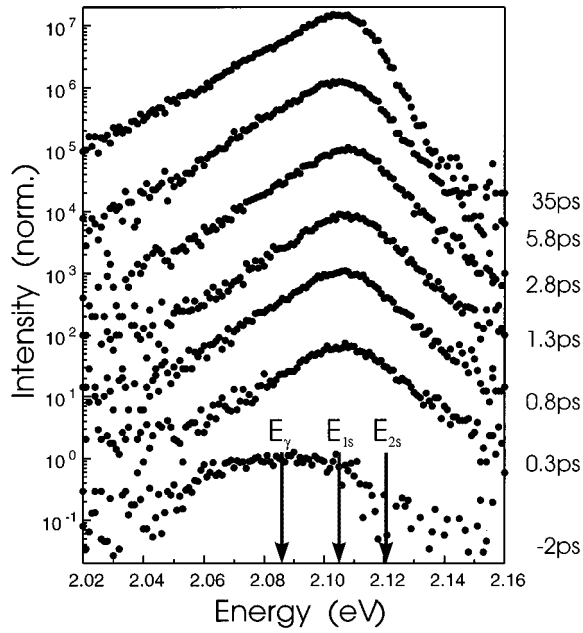


FIG. 2. Time-resolved luminescence spectra of GaSe recorded for delay times from -2 to 35 ps. To avoid intersections along the vertical axis, the spectra are shifted to each other. The spectral positions of the $1s$ - and $2s$ -free excitons and the localized exciton γ at energy E_γ are marked by arrows.

pairs. This part of the PL spectra can be described by Boltzman statistics. Ultrafast carrier thermalization occurs on a time scale shorter than the time resolution of the measurements. By fitting the high-energy tails of the spectra with Boltzman distributions the effective carrier temperature T_C as a function of time (see Fig. 3) can be derived. The cooling curve $T_C(t)$ reveals a fast and a slow energy loss stage of the carriers. The excess energy of the photoexcited carriers corresponds to the initial carrier temperature of ~ 5670 K, and the highest effective carrier temperature derived from the luminescence spectra is less than 300 K. Therefore a significant amount of the excess energy is transferred from the carriers to the phonon system already within a

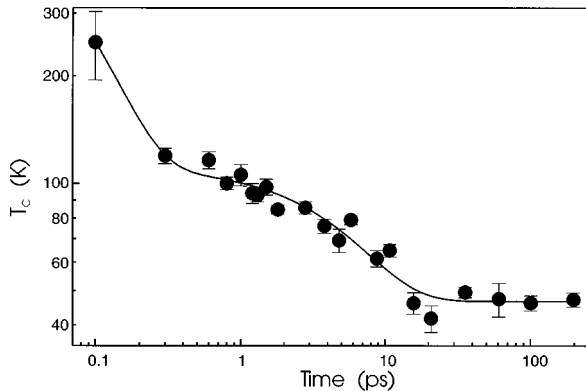


FIG. 3. Double logarithmic plot of the effective carrier temperature as a function of the delay time after excitation. The data points shown by solid circles are derived by fitting of high-energy slopes ($E > E_{\text{gap}}$) of the time-resolved PL spectra using Boltzman statistics. The solid line is a double exponential decay fitted to the data points.

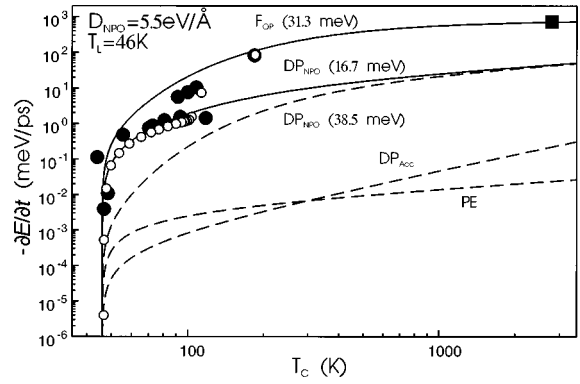


FIG. 4. Symbols: Measured carrier energy relaxation rates as a function of the effective carrier temperature [solid circles, derived from the measured cooling curve; open circles, derived from the double exponential fit to the measured data points; solid square, estimated value for the subpicosecond carrier cooling from 5670 to 100 K (using a time range of 1 ps and an average carrier temperature of ~ 2800 K)]. Lines: Calculated carrier energy relaxation rates. Solid lines: Dominant relaxation rates [F_{OP} (31.3 meV), Fröhlich coupling to the polar longitudinal optical $E'(2^2)$ phonon mode (31.3 meV); DP_{NPO} (16.7 meV), deformation potential coupling to the nonpolar optical $A'_1(1^2)$ phonon mode (16.7 meV)]. Dashed lines: Relaxation rates of minor significance [DP_{NPO} (38.5 meV), deformation potential coupling to the nonpolar optical $A'_1(2^2)$ phonon mode (38.5 meV); DP_{Acc} , deformation potential coupling to acoustic phonons; PE , piezoelectric coupling].

time shorter than the time resolution of the measurement (150 fs). Even though the fast initial cooling cannot be followed in great detail the presence of the subpicosecond relaxation stage is observed by the rapid carrier cooling from ~ 300 to ~ 100 K (see Fig. 3). This stage is followed by a slower picosecond cooling of the carriers down to the lattice temperature. The observed cooling dynamics can be well described by a double exponential decay with time constants 0.1 and 5.7 ps. The lattice temperature T_0 is thereby determined to 46 K.

To identify the dominant carrier energy loss mechanisms in GaSe, the cooling rates of electron hole pairs are extracted from the cooling dynamics. The experimental results are compared with the relaxation rates calculated for the different types of carrier-phonon interactions, such as the long-range Fröhlich interaction with the longitudinal optical 31.3 meV phonon, the deformation-potential coupling of the carriers to the nonpolar optical A'_1 phonons (16.7 and 38.5 meV), and the acoustic phonons and the piezoelectric coupling to the acoustic phonons.^{1,32,33} The analysis is performed at a lattice temperature of $T_0 = 46$ K, using the GaSe parameters from Refs. 11,27,34. The resulting plots are shown in Fig. 4, where the high temperatures correspond to early times after excitation.

Two different energy-loss mechanisms for the fast and the slow relaxation stage of the carrier cooling are identified. The cooling rate during the first picosecond at temperatures between 5670 and 100 K approaches the values calculated for the Fröhlich coupling to the longitudinal optical $E'(2^2)$ phonon (31.3 meV). The corresponding cooling rate is given by the following expression:^{1,32,33}

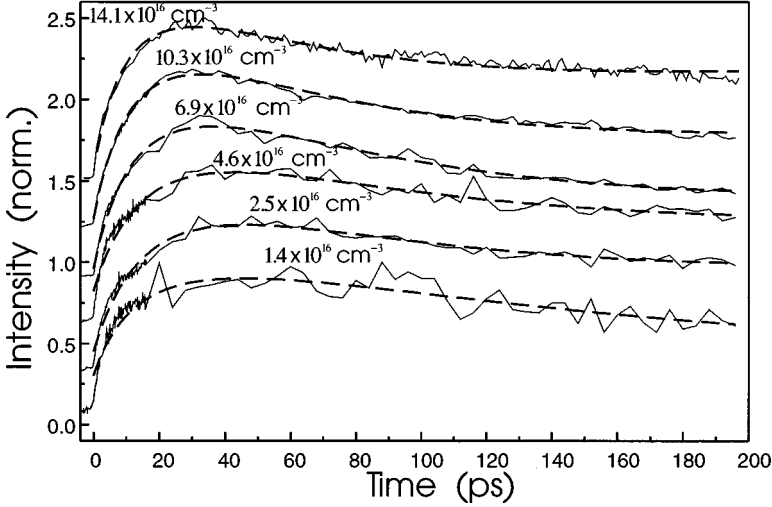


FIG. 5. *Solid lines*: Luminescence time transients taken at the spectral position of the $1s$ exciton for different carrier densities. *Dashed lines*: Fit to the data using the rate equation model described in the text. The curves are normalized and offset for clarity.

$$\begin{aligned}
 -\frac{\partial E}{\partial t} [\text{meV/ps}] &= 354 \times \left(\frac{m^*}{m_0}\right)^{1/2} \left(\frac{1}{\epsilon_\infty} - \frac{1}{\epsilon_0}\right) \\
 &\times (\hbar\omega_{[\text{meV}]})^{3/2} \frac{e^{(\chi_0 - \chi_c)} - 1}{e^{\chi_0} - 1} \\
 &\times \left(\frac{\pi}{2}\right)^{-1/2} \left(\frac{\chi_c}{2}\right)^{1/2} e^{\chi_c/2} \times K_0\left(\frac{\chi_c}{2}\right),
 \end{aligned}$$

where $\chi_0 = \hbar\omega/k_B T_0$ and $\chi_c = \hbar\omega/k_B T_c$. T_c and T_0 are the effective carrier temperature and lattice temperature, respectively, $\hbar\omega$ is the energy of the polar optical $E'(2^2)$ phonon, m^* is the reduced mass of the electron hole pairs, ϵ_0 and ϵ_∞ are the static and optical dielectric constants, respectively, and K_0 is the modified Bessel function of zero order.

For delay times longer than 1 ps, the experimentally measured cooling rates get clearly smaller than those for the Fröhlich interaction. They finally approach the values being characteristic of deformation potential coupling of the nonpolar optical $A_1'(1^2)$ phonon (16.7 meV). The slow cooling dynamics of the electron hole pairs ($t \geq 1.5$ ps, $T_c \leq 100$ K) are well described by interaction with nonpolar optical $A_1'(1^2)$ phonons (16.7 meV), whereas the rates calculated for other carrier-phonon coupling mechanisms deviate by at least an order of magnitude from the measured values. The carrier energy relaxation rate for the interaction with the nonpolar optical phonon due to deformation potential coupling is given by^{11,1,32,33}

$$\begin{aligned}
 -\frac{\partial E}{\partial t} [\text{meV/ps}] &= 3.553 \times \frac{(m^*/m_0)^{3/2} D^2_{[\text{eV/\AA}]}}{\rho_{[\text{g/cm}^3]}} \\
 &\times (\hbar\omega_{[\text{meV}]})^{1/2} \frac{e^{(\chi_0 - \chi_c)} - 1}{e^{\chi_0} - 1} \\
 &\times \left(\frac{\pi}{2}\right)^{-1/2} \left(\frac{\chi_c}{2}\right)^{1/2} e^{\chi_c/2} \times K_1\left(\frac{\chi_c}{2}\right),
 \end{aligned}$$

where $\hbar\omega$ is the energy of the nonpolar optical $A_1'(1^2)$ phonon, ρ is the modified crystal density,^{5,8,11} D is the deformation potential constant, and K_1 is the modified Bessel function of the first order. Using a deformation potential constant

D_{NPO} of 5.5 eV/Å in this formula fits the measured data best. This result corresponds well with the values for D_{NPO} of 5.5–6.6 eV/Å reported in Refs. 6,8,10. The slight differences can be due to a weak screening of the deformation potential coupling by the excited carriers in the present study.

We attribute the reduction in the efficiency of the polar carrier-phonon interaction to the buildup of nonequilibrium phonon populations, which can develop on the subpicosecond timescale as demonstrated in Ref. 3. Estimations show that the threshold for saturation of the $E'(2^2)$ phonon mode is at carrier densities of $\sim 5 \times 10^{16} \text{ cm}^{-3}$, which is in the range of the excitation densities used in the present experiments.³⁵

B. Exciton formation dynamics

As was pointed out, the carrier energy relaxation is accompanied by the shift of the PL maximum towards the position of the free $1s$ exciton. This behavior shows the buildup of the excitonic state population due to the carrier cooling, and is an incoherent formation process of free excitons from the thermalized electron hole pairs.

The free-exciton formation rate is determined by the exciton binding energy ($E_B^X = 19$ meV in GaSe) and the thermal energy of the carriers $\frac{3}{2}k_B T_c$. When the thermal energy of the carriers becomes smaller than the exciton binding energy, the attractive Coulomb interaction between electrons and holes is strong enough to bind them into excitons and prevent the thermal dissociation of the exciton. This leads to an efficient formation process of excitons. As the exciton formation results from the electron hole interaction the formation rate increases with increasing carrier density. According to our data, within the first picosecond after excitation the thermal energy of the carriers becomes smaller than the exciton binding energy, suggesting the efficient exciton formation at delay times $t \geq 1$ ps.

We studied exciton formation dynamics by analyzing PL time transients recorded at the spectral position of the free $1s$ -exciton resonance for different excitation densities (see Fig. 5). The transients have a finite rise time τ_X , which is attributed to the exciton formation time. The formation rate of free excitons $\gamma_X = 1/\tau_X$ increases with increasing carrier density, as expected from the above model.

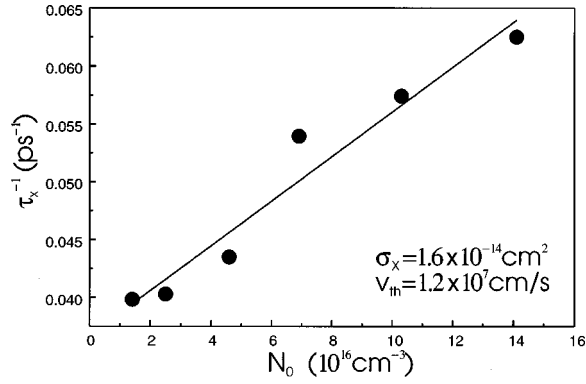


FIG. 6. Excitation density dependence of the free-exciton formation rate (solid circles) derived by fitting PL time transients recorded at the position of the $1s$ -exciton resonance along with a linear fit (solid line). The slope of the straight line $\sigma_X v_{th}$ is $1.93 \times 10^{-7} \text{ cm}^3/\text{s}$ and corresponds to the exciton formation cross section σ_X of $1.6 \times 10^{-14} \text{ cm}^2$.

To analyze the measured dynamics in a quantitative way, we use a set of two coupled rate equations, which describe the temporal evolution of the electron hole pair $[C(t)]$ and exciton density $[X(t)]$.^{26,22} The model implies that electron and hole densities develop equally in time, and the carrier density decays solely due to the formation of excitons:

$$\begin{aligned} \frac{\partial}{\partial t} \left(\frac{C(t)}{N_0} \right) &= -\gamma_X \times \left(\frac{C(t)}{N_0} \right)^2, \\ \frac{\partial}{\partial t} \left(\frac{X(t)}{N_0} \right) &= +\gamma_X \times \left(\frac{C(t)}{N_0} \right)^2 - \frac{1}{\tau_D} \times \left(\frac{X(t)}{N_0} \right), \\ \left(\frac{C(t=0)}{N_0} \right) &= 1, \end{aligned}$$

where N_0 is the initially excited electron hole pair density. $\gamma_X = \sigma_X v_{th} \times N_0$ is the free-exciton formation rate, where σ_X is the free-exciton formation cross section, and v_{th} is the thermal velocity of the carriers. τ_D accounts for the decay of the excitonic PL, which is mainly determined by the energy relaxation of the free excitons due to localization as discussed below. As the thermal dissociation of excitons has a

negligible small effect on the dynamics at $t \geq 1 \text{ ps}$ the corresponding term is not included in the rate equations.²⁶

The measured data are well described by the above model, as illustrated by the fitting curves in Fig. 5. The exciton formation rates are chosen to yield the best fit to the data, and are shown by solid circles in Fig. 6. In agreement with the formula $\gamma_X = \sigma_X v_{th} \times N_0$ the exciton formation rate increases linearly with the excitation density, which is shown by the straight line in Fig. 6. Using the value of the average thermal carrier velocity v_{th} of $1.2 \times 10^7 \text{ cm/s}$ (corresponding to the measured average effective carrier temperature of 48 K) the cross section σ_X for free-exciton formation is determined to $1.6 \times 10^{-14} \text{ cm}^2$, from the slope of the straight line.

To study the exciton trapping dynamics, we recorded PL time transients at the spectral position of the bound exciton at E_γ (see Fig. 1). These are compared in Fig. 7 to those recorded at the position of the $1s$ -free-exciton resonance and at spectral energies above the band gap. We observe a significant increase of the luminescence rise time with decreasing detection energy, which is consistent with the spectral migration of excitons observed previously.²²⁻²⁵ The rise time of ~ 25 and ~ 35 ps of the transients recorded at 2.08 and 2.06 eV, respectively can be taken as a measure of the trapping time of free excitons at stacking faults in GaSe, which is in agreement with previously published results.²⁴

IV. CONCLUSIONS

A comprehensive study of the carrier cooling and exciton formation dynamics in GaSe has been performed using femtosecond time-resolved PL measurements. Very fast initial energy relaxation of carriers on the subpicosecond time scale is explained by the Fröhlich coupling to the longitudinal optical $E'(2^2)$ phonons in GaSe. The slowing down of the cooling dynamics at delay times $t \geq 1 \text{ ps}$ is attributed to the buildup of a nonequilibrium population of the longitudinal optical $E'(2^2)$ phonon mode, developing on the subpicosecond time scale. The dominating energy-loss mechanism for the subsequent slower cooling dynamics

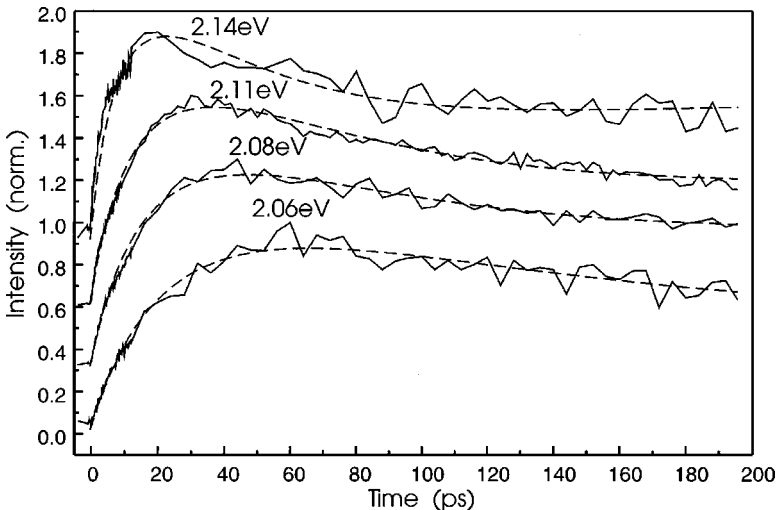


FIG. 7. *Solid lines*: PL time transients recorded at different spectral positions. The curves are arbitrary offset for clarity. *Dashed lines*: Simple fit to the data to determine the rise times of the PL transients.

is the deformation potential coupling of the carriers to the nonpolar optical $A_1'(1^2)$ phonon. The deformation potential coupling constant found by the modeling of the data is determined to be 5.5 eV/\AA , which is in close agreement with the values derived by other experimental techniques. The studies of excitation density-dependent exciton formation dynamics indicate the free-exciton formation cross section σ_X of $1.6 \times 10^{-14} \text{ cm}^2$. The dynamics of the bound

exciton related PL show that exciton trapping occurs on a timescale of $\sim 30 \text{ ps}$.

ACKNOWLEDGMENTS

This work has been supported by the Deutsche Forschungsgemeinschaft (Ku540/16-1).

- ¹J. Shah and R.F. Leheny, *Semiconductors Probed by Ultrafast Laser Spectroscopy*, edited by R.R. Alfano (Academic, Orlando, FL, 1984), pp. 45–75.
- ²J. Shah, *Ultrafast Spectroscopy of Semiconductors and Semiconductor Nanostructures*, edited by M. Cardona, Springer Series in Solid-State Sciences Vol. 115 (Springer, Berlin, 1996), pp. 133–193.
- ³V. Klimov, P. Haring Bolivar, and H. Kurz, *Phys. Rev. B* **52**, 4728 (1995).
- ⁴R.C. Fivaz, *Nuovo Cimento B* **63**, 10 (1969).
- ⁵P. Schmid, *Nuovo Cimento B* **21**, 258 (1974).
- ⁶M. Schlüter, *Nuovo Cimento B* **13**, 313 (1973).
- ⁷V. Augelli, C. Manfredotti, R. Murri, and L. Vasanelli, *Phys. Rev. B* **17**, 3221 (1978).
- ⁸P. Schmid and J.P. Voitchovsky, *Phys. Status Solidi B* **65**, 249 (1974).
- ⁹G. Antonioli, D. Bianchi, U. Emilliani, and P. Podini, *Nuovo Cimento B* **54**, 211 (1979).
- ¹⁰N. Piccioli and R. Le Toullec, *J. Phys. (France)* **50**, 3395 (1989).
- ¹¹S.S. Yao, J. Buchert, and R.R. Alfano, *Phys. Rev. B* **25**, 6534 (1982).
- ¹²S.S. Yao and R.R. Alfano, *Phys. Rev. B* **26**, 4781 (1982).
- ¹³S.S. Yao and R.R. Alfano, *Phys. Rev. B* **27**, 2439 (1983).
- ¹⁴V. Capozzi, L. Pavesi, and J.L. Staehli, *J. Lumin.* **48** **49**, 111 (1991).
- ¹⁵L. Pavesi, J.L. Staehli, and V. Capozzi, *Phys. Rev. B* **39**, 10 982 (1989).
- ¹⁶J. Kusano, Y. Segawa, Y. Aoyagi, and S. Namba, *Phys. Rev. B* **40**, 1685 (1989).
- ¹⁷R. Kumar, A.S. Vengurlekar, S.S. Prabhu, J. Shah, and L.N. Pfeiffer, *Phys. Rev. B* **54**, 4891 (1996).
- ¹⁸D. Robart, X. Marie, B. Baylac, T. Amand, M. Brousseau, G. Bacquet, G. Debart, R. Planel, and J.M. Gerard, *Solid State Commun.* **95**, 287 (1995).
- ¹⁹T.C. Damen, J. Shah, D.Y. Oberli, D.S. Chemla, J.E. Cunningham, and J.M. Kuo, *Phys. Rev. B* **42**, 7434 (1990).
- ²⁰B. Dareys, X. Marie, T. Amand, B. Baylac, J. Barrau, I. Razdobreev, M. Brousseau, and D. Dunstan, *Solid State Commun.* **90**, 237 (1994).
- ²¹H. Schneider, K. Kanamoto, and K. Fujiwara, *Appl. Phys. Lett.* **66**, 905 (1995).
- ²²R.A. Taylor and J.F. Ryan, *J. Phys. C* **20**, 6175 (1987).
- ²³X.C. Zhang, M. Gal, and A.V. Nurmikko, *Phys. Rev. B* **30**, 6214 (1984).
- ²⁴V. Mizeikis, V.G. Lyssenko, J. Erland, and J. M. Hvam, *Phys. Rev. B* **51**, 16 651 (1995).
- ²⁵F. Minami and K. Era, *Phys. Rev. B* **35**, 2509 (1987).
- ²⁶V.S. Dneprovskii, V.I. Klimov, and M.G. Novikov, *Zh. Éksp. Teor. Fiz.* **99**, 843, (1991) [*Sov. Phys. JETP* **72**(3), 468 (1991)].
- ²⁷*Physics of Non-Tetrahedrally Bonded Binary Compounds*, edited by K.H. Hellwege and O. Madelung, Landolt-Börnstein, New Series, Group III, Vol. 17, Pt. f (Springer, Berlin, 1983).
- ²⁸A. Chevy, A. Kuhn, and M.S. Martin, *J. Cryst. Growth* **38**, 118 (1977).
- ²⁹J.J. Staehli and A. Frova, *Physica B* **99**, 299 (1980).
- ³⁰J.P. Voitchovsky and A. Mercier, *Nuovo Cimento B* **22**, 273 (1975).
- ³¹R. Sporcken, R. Hafsi, F. Coletti, J. M. Debever, P.A. Thiry, and A. Chevy, *Phys. Rev. B* **49**, 11 093 (1994).
- ³²E.M. Conwell, in *Solid State Physics: Advances in Research and Applications*, edited by F. Seitz, D. Turnbull, and H. Ehrenreich (Academic, New York, 1967), Vol. 9, Chap. 3.
- ³³S.M. Kogan, *Fiz. Tverd. Tela* **4**, 2474, (1962) [*Sov. Phys. Solid State* **4**, 1813 (1963)].
- ³⁴G.I. Abutalybov, S.Z. Dzhafarova, and N.A. Ragimova, *Phys. Rev. B* **51**, 17 479 (1995).
- ³⁵V.S. Dneprovskii *et al.*, *Pis'ma Zh. Éksp. Teor. Fiz.* **52**, 1130 (1990) [*JETP Lett.* **52**, 534 (1990)].